Active sensing methods of ionic polymer metal composite (IPMC)
Comparative study in frequency domain

Mohd Isa, Wan Hasbullah; Hunt, Andres; Hossein Nia Kani, Hassan

DOI
10.1109/ROBOSOFT.2019.8722790

Publication date
2019

Document Version
Accepted author manuscript

Published in
2019 IEEE International Conference on Soft Robotics (RoboSoft 2019)

Active Sensing Methods of Ionic Polymer Metal Composite (IPMC): Comparative Study in Frequency Domain

WanHasbullah MohdIsa[1], Andres Hunt[2] and S. Hassan HosseinNia[2]

***Abstract*— Ionic polymer-metal composites (IPMCs) are soft transducers that bend in response to low-voltage input, and generate voltage in response to deformations. Their potential applications include compliant locomotion systems, small-scale robotics, energy harvesting and biomedical instrumentation. The materials are inherently compliant, simple to shape, simple to miniaturize and simple to integrate into a system. Compared to actuation, IPMC sensing has not been intensively studied. The existing reports focus on the sensing phenomenon, but provide insufficient characterization for implementation purposes. This work aims to address this gap by studying and comparing the frequency responses and noise dynamics of different IPMC active sensing signals, i.e. voltage, charge and current. These characteristics are experimentally identified by mechanically exciting IPMC samples, and simultaneously measuring the respective signals and material deformations. The results provide a systematic comparison between different implementations of active sensing with IPMCs, and give insights into their strengths and limitations.**

I. INTRODUCTION

Mechatronic systems that need to be mechanically compliant either partially or entirely are applied in many applications such as compliant locomotion systems, small-scaled robotics, energy harvesting and biomedical instrumentation. Such systems require not only soft 'body' but also actuators and sensors that are inherently compliant, simple to shape, simple to miniaturize and simple to integrate [1]. These characteristics are inherent to several bending smart materials, e.g. piezopolymers (PVDF [2], its copolymer [3] and its highly electrostrictive terpolymer [4]), piezoceramic patches [5], dielectric elastomers [6], conductive polymer [7], and ionic polymer metal composites (IPMCs) [8]. IPMCs are more attractive with respect to other bending smart materials for this kind of applications, since they require low actuation voltages, have reasonable actuation bandwidth, and produce large deformations [8]. While IPMC actuation has been studied extensively and proposed for many applications [9], the sensing abilities have gained much less attention. Since the discovery of IPMCs' sensing capabilities in 1992 [10], the reported studies have used black-box models [11], [12], [13], grey-box models [14], [15], [16] and white-box models [17], [18], [19], [20], [21], [22], [23], [24], [25] to describe their sensing dynamics. The reported application studies have investigated exploiting them as translational [11], rotational [26], and omnidirectional [27] position sensors, velocity sensors [28], wall shear stress sensors [29], seismic sensors [30], vibration sensors [31], force sensors [32], flow sensors [33], humidity sensors [34], and wearable pulse and braille sensors [35]. Sensing with IPMCs can be realized by several means i.e. measuring voltage [36], [37], [38], [39], [40], current [37], [19], [41], [31], [25], [42], [43], charge [37], [44], [29], [45], [46], and the impedance change [47], [48].

These means can be grouped into active and passive sensing methods. Active sensing is based on signals generated by IPMC in response to deformation where uneven distribution of charge across material thickness generates potential difference between its electrodes as illustrated in Fig. 1 [36]. Voltage is measurable between IPMC electrodes using high input impedance voltage measurement circuitry, current is measurable using low impedance circuit that provides virtual short-circuit, and charge is measured by means of displaced charge from IPMC electrode into the measurement circuitry. On the other hand, passive sensing is based on impedance change: either in asymmetrically deformed electrodes of IPMCs due to bending [48], or capacitance change between IPMC electrode and an external electrode [47]. Relying on the observations in the previously discussed reports, active sensing is more suitable for dynamic sensing, and passive sensing is more reliable for static and quasi-static sensing.

Despite reported efforts towards modelling and implementations of different IPMC sensing methods, the implementa-

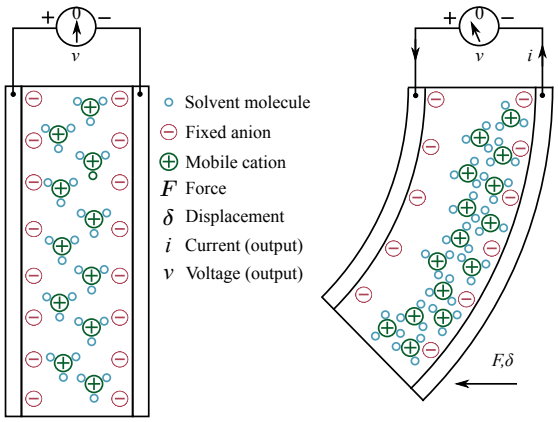

Fig. 1. Sensing phenomenon inside IPMC. Motion of mobile counterions generates charge accumulation on the electrode layers.

[1]WanHasbullah MohdIsa is with Department of Precision and Microsytems Engineering, Faculty of Mechanical, Maritime and Materials Engineering, Delft University of Technology, 2628 CD Delft, The Netherlands and Faculty of Manufacturing Engineering, Universiti Malaysia Pahang, 26600, Pekan, Pahang Malaysia w.h.b.mohdisa@tudelft.nl or wanhasbullah@ump.edu.my

[2]Andres Hunt and S. Hassan HosseinNia are with Department of Precision and Microsytems Engineering, Faculty of Mechanical, Maritime and Materials Engineering, Delft University of Technology, 2628 CD Delft, The Netherlands A.Hunt-1@tudelft.nl and S.H.HosseinNiaKani@tudelft.nl

tions vary between reports and are laconic in descriptions. Usable frequency ranges are not analysed and different sensing methods cannot be compared due to inconsistencies in implementations and used materials. Furthermore, the inconsistent displacements between the previous reports and also over the entire experimented frequency range in each of them complicate the comparison.

Therefore, this work aims to address these gaps by improving the sensing characterization procedure of IPMC as well as comparing the frequency responses and noise characteristics of voltage, current and charge measurements under identical conditions. The characterization improvement is achieved by assuring constant displacement amplitude of IPMCs at all tested frequencies. Characteristics of each sensing signals are experimentally identified by mechanically exciting IPMC samples, and simultaneously measuring the respective signals. The results provide a systematic comparison of IPMC sensing methods, preliminary guidelines for selection and implementation of active sensing methods, and give insights into their strengths and limitations.

II. METHODOLOGY

In order to systematically characterize and compare all IPMC active signals in the frequency domain, we need to provide sinusoidal bending motion to IPMC, simultaneously measure the generated signals and further process them. Therefore, the experimental set-up is designed to achieve these goals, and it comprises of: mechanical excitation system, described in section II-A, and signal conditioning circuits, described in section II-B. Processing of the results is explained in section II-C. Block diagram of the experimental set-up is shown in Fig. 2 and illustrated in photo in Fig. 3.

The used IPMC materials are made of Nafion polymer and coated with platinum electrodes. Their total thickness is approximately 200 μm. Materials are ion-exchanged into sodium form and use water as solvent. The dimensions of IPMC samples are 10 *mm* by 30 *mm*.

A. Mechanical Excitation System

The mechanical excitation system is shown in Fig. 3 and is constructed as follows. Measurements are controlled by a PC computer from Matlab 2017a environment through a NI USB 6211 data acquisition board (A). To excite the IPMC sample, we use the B&K Type 4801 shaker (D), whose current input is converted and amplified from voltage output of the data acquisition board by a custom-made voltage amplifier (B) and TIRA Type BAA 120 power amplifier (C). The tip displacements are measured using two Opto NCDT 1420 laser triangulation sensors (G) that work at 2 kHz sampling rate, and are powered from a 24 V power supply (H). IPMC deformation is equal to the difference between these displacement measurements.

The mechanical excitation system has to periodically bend the IPMC sample with a consistent amplitude and deformation profile over the entire range of the investigated frequencies. This requires at all frequencies (a) consistent excitation amplitude from the shaker, (b) consistent displacement between IPMC tips, and (c) consistent IPMC deformation profile. This is necessary to minimize non-linearities that stem from non-uniform deformation amplitudes over the investigated frequency range. Therefore, (a) we identify the dynamics of our excitation system as shown in Fig. 4 and use its inverse model to compensate for non-uniformity in displacement amplitudes at different frequencies. This also assures sufficient bending amplitudes at low frequencies that otherwise decrease due to the high-pass behavior of the excitation system. With current shaker, this allows us to achieve consistent displacement of 1.8 *mm* peak-to-peak at frequencies above $0.08Hz$ as depicted in Fig. 5. We observed that the shaker provides somewhat different displacement amplitudes in positive and negative directions (Fig. 5), but this is not expected to significantly influence the dynamic measurements in this study. (b) In order to assure that displacement between IPMC tips is always equal to shaker displacement, we use the following setting. Shaker provides mechanical excitation to the base of the IPMC beam, while the other end of the IPMC is constrained from moving horizontally by a low-friction pin-in-a-slot joint (see Fig. 3 (ii)). (c) IPMC sensors are most commonly bent in their first cantilever mode. This is necessary to maximize signal strength and avoid signal cancellation that could occur due to reciprocal curvature over the same IPMC sample. In order to assure that higher mode shapes are not excited, we need to add stiffness to the system, effectively raising the first resonance frequency above the investigated frequency range. This is realized by coupling the IPMC with two leaf springs in parallel. Thickness and widths of these springs are 0.10 *mm* and 7 *mm* respectively, and the free length of springs and IPMC is 22 *mm*.

The experiments are conducted at 25 different frequencies, logarithmically distributed over the frequency range of 0.08 Hz to 60 Hz. Each signals is applied for at least 5 cycles and 4s in order to ensure that enough measurement data is collected. At every frequency, required voltage amplitudes to provide 1.8 *mm* displacement on the IPMC sample are calculated from the inverse model of shaker system dynamics (see Fig. 4). Each measurement is repeated five times to ensure reliable results. The experiments are conducted in open air. The ambient temperature is between 21 $^{\circ}C$ and 25 $^{\circ}C$, while the surrounding relative humidity level is 45 %.

B. Signal Conditioning Circuits

This section explains the three signal conditioning circuits that are used to measure the voltage, current, and charge of the IPMC sample in response to deformation. Principle designs of these circuits are shown in Figs. 6, 7, and 8 respectively. Their overall frequency responses are experimentally identified, and shown in Fig. 4. These amplifier circuits are shielded by a metal box (F in Fig. 3).

The first sensing methodology bases on measuring the voltage difference that is created between the IPMC electrodes. IPMC is connected to the sensing circuit with very high input impedance, as illustrated in Fig. 6. High input

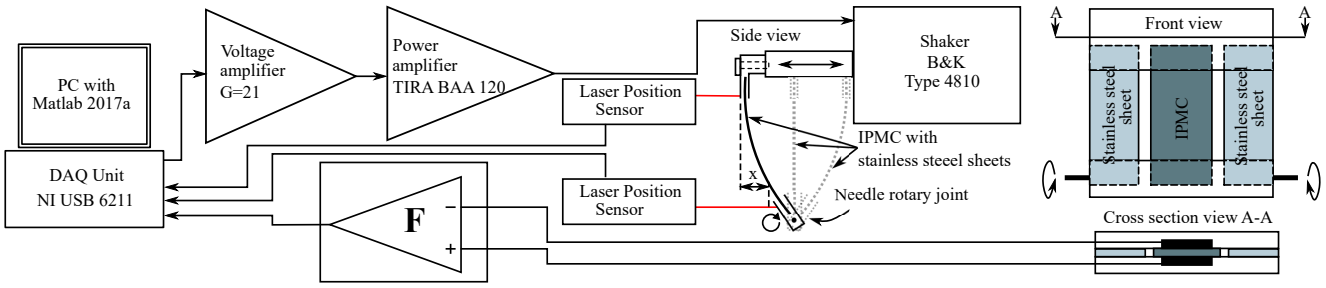

Fig. 2. Schematic view of the experimental setup. "F" is an interchangeable amplifier circuit that is either voltage amplifier ($G = 56000$), current amplifier ($G = 116000$) or charge amplifier ($f_c = 15Hz$ and high frequency gain of 10^{11}).

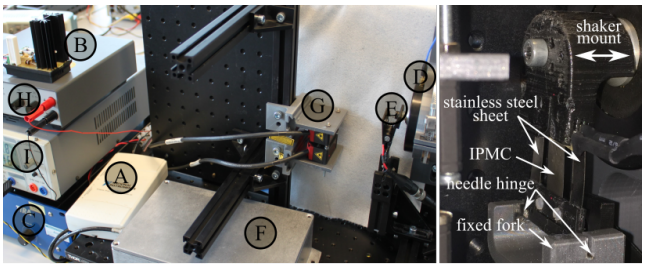

(i) (ii)

Fig. 3. Experimental setup. In (i), 'A' is data acquisition board, 'B' is voltage amplifier, 'C' is power amplifier, 'D' is shaker, 'E' is IPMC clamp, 'F' is metal box containing measurement circuit, 'G' is laser triangulation sensors, and 'H' and 'I' are power supplies. (ii) Close-up photo of the experimental setup 'E'.

impedance is characteristic to voltage measurements, and it is required to minimize voltage drop due to the measurement circuitry. In this work, the voltage amplifier with the gain of 56000 V/V is used and its experimentally identified bode plot is shown in Fig. 4.

The second sensing methodology bases on measuring the current that flows through the measurement circuit to maintain zero voltage between its electrodes. A sensing circuit with very low input impedance connects IPMC electrodes as shown is Fig. 7 and cancels the voltage generate by the material. A two-staged current amplifier with the total gain of 116000 V/A is used in these measurements, and its bode plot is depicted in Fig. 4.

The third sensing methodology bases on measuring the charge on the electrodes of IPMC. For that, we need a high input impedance amplifier with a capacitor in the feedback line, where the charge from IPMC flows to. For implementation, an additional high-Ohm resistor is required in parallel with this capacitor. The principle design of this circuit is shown in Fig. 8. In this work, a two-staged charge amplifier is used with a cut-off frequency of $15Hz$ and gain of 10^9 V/C. Its experimentally identified bode plot is shown in Fig. 4.

C. Signal Processing

This section explains the signal processing that is performed on the measurements to obtain the frequency responses, coherences, and signal power ratio in the measurement (PR).

Frequency responses are obtained using 'tfestimate' function in Matlab. It calculates the quotient between the cross power spectral densities of IPMC displacement and the signals, (P_{sx}), and power spectral densities of IPMC displacement, P_{xx} as follows:

$$TF(\omega) = \frac{P_{sx}(\omega)}{P_{xx}(\omega)} \tag{1}$$

Coherences are estimated using 'mscohere' function in Matlab. It calculates the quotient that shows correlations between the measured sensing signals and IPMC displacement:

$$C(\omega_i) = \frac{|\, P_{sx}(\omega_i)\,|^2}{P_{xx}(\omega_i) P_{ss}(\omega_i)} \tag{2}$$

PRs are obtained by calculating the fraction of power of the excited frequency $P(\omega_i)$ with respect to total power of the signal within the frequency interval of 0.01 Hz to 100 Hz:

$$PR(\omega_i) = \frac{P(\omega_i)}{\sum_{0.01\ Hz}^{100\ Hz} P(\omega_i)} \tag{3}$$

This figure provides relative indication of how much the mechanical excitation frequency of IPMC contributes to the total power in the measured signal.

III. RESULTS AND DISCUSSION

This section discusses the results of experiments described in section II which are shown in Fig. 9. The discussion is divided into three frequency ranges: (1) low-frequency (0.08 Hz to 1 Hz), (2) mid-frequency (1 Hz to 10 Hz), and (3) high-frequency ($10Hz$ to $60Hz$).

A. Low-frequency range

As shown in Fig. 9, the magnitudes of voltage and current increase with the frequencies at approximately $+1$ slope in logarithmic scale. Magnitude of the charge amplifier reading also increases gradually but with a lower slope. This is caused by the high-pass filter behaviour of charge amplifier. Similarly to [37], this is corrected by multiplying the measurement with the inverse transfer function of the charge sensing circuit shown in Fig. 4. Corrected magnitude of the frequency response of charge measurement decreases with frequency at approximately -1 slope in logarithmic scale.

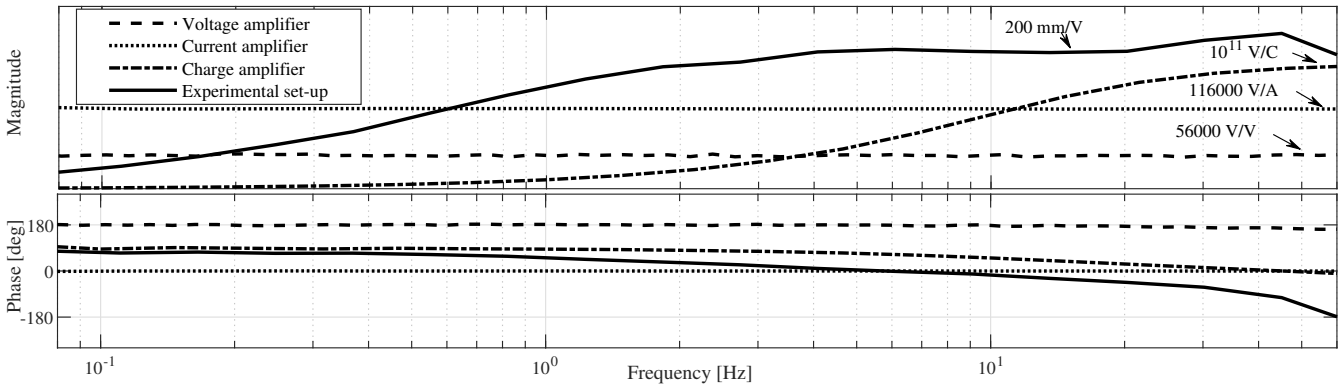

Fig. 4. Bode plots of the mechanical system, voltage, current and charge amplifiers. The gains of voltage and current amplifiers are 56000 and 116000 respectively. The cut-off frequency of charge amplifier is 15 Hz and its high frequency gain is 10^{11}.

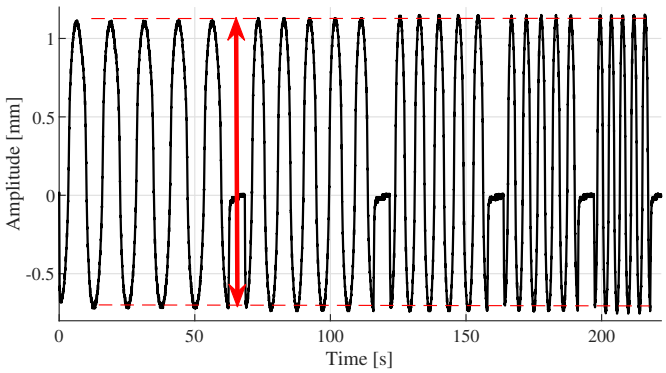

Fig. 5. An example of IPMC deformation during experiments. Displacement is constant over all experiments.

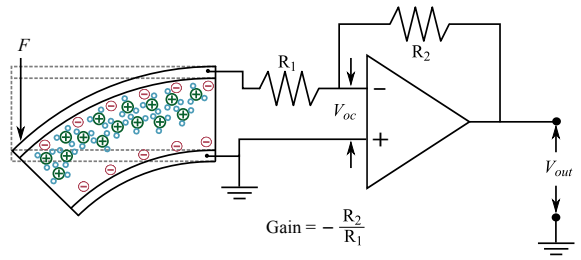

Fig. 6. Principle design of the voltage amplifier circuit and its coupling to IPMC.

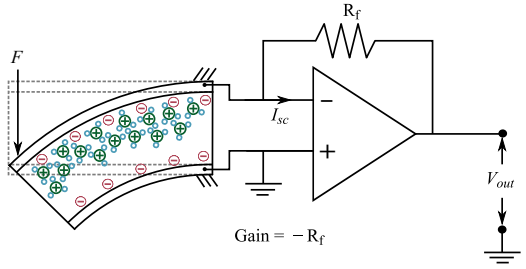

Fig. 7. Principle design of the current amplifier circuit and its coupling to IPMC.

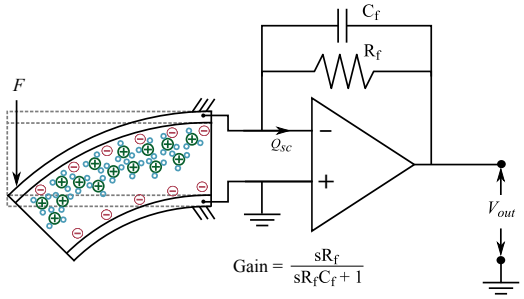

Fig. 8. Principle design of the charge amplifier circuit and its coupling to IPMC.

The phase of the charge measurements are really close to 0° over all frequencies, while those of current and voltage remain close to 50° and 65° respectively.

Current measurements show slightly better coherences with displacement than voltage measurements, while coherences of both these measurements increase with frequency, reaching approximately 1 at 0.5 Hz. Charge measurements show close to zero correlations, indicating that these readings are unusable for sensing within this frequency range. The latter is caused by the high pass filter effect of the charge amplifier.

All the PRs are observed to slightly increase with frequency. While PRs for current measurements are very slightly better than these of voltage measurements, both show roughly two times better figures than charge measurements.

From these observations, the most suitable sensing signal for low frequency operating range is short circuit current. It provides high signal magnitude, good coherence, and relatively strong signal with respect to noise. Voltage measurement has slightly inferior performance with respect to current, but it is significantly better than charge signal that is strongly dominated by noise. Voltage measurement circuits are simplest to implement, while implementations of current and charge sensing electronics are somewhat more complex.

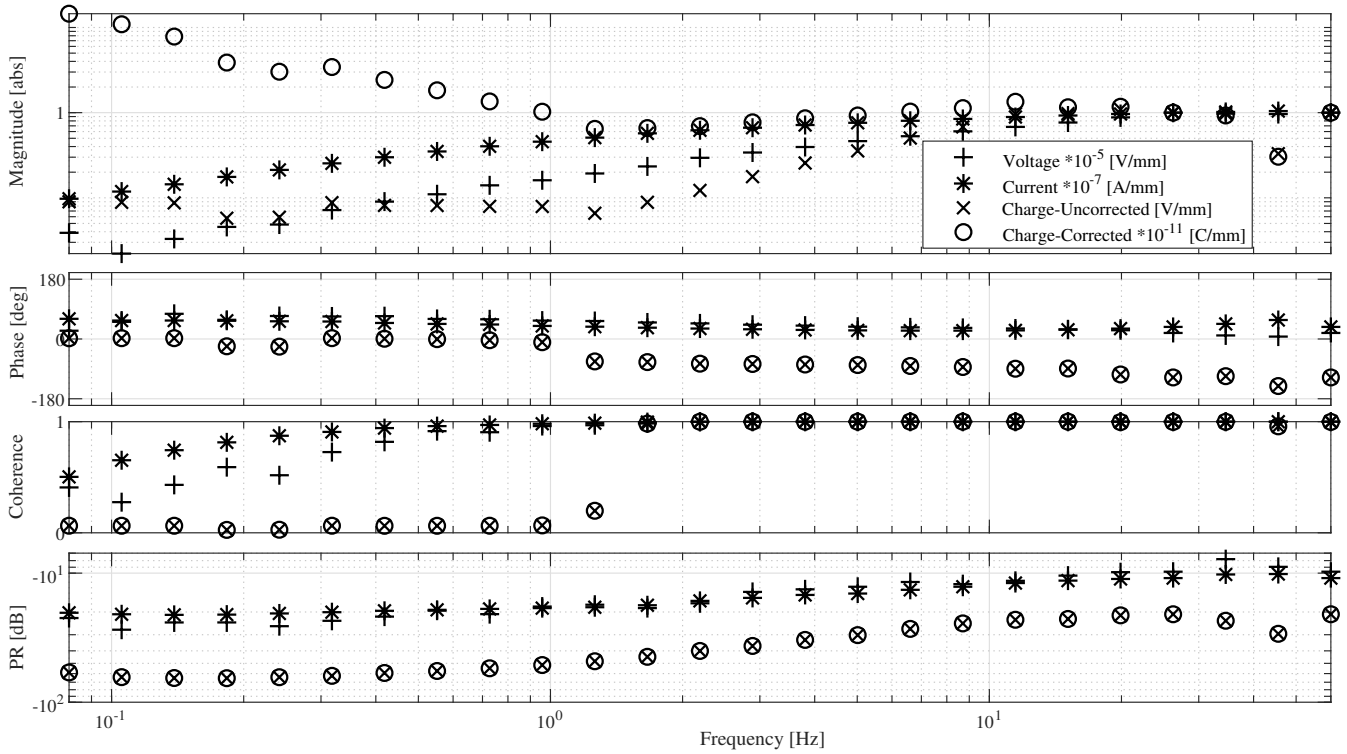

Fig. 9. Bode plot, coherence and PR results of IPMC active sensing signals in response to IPMC displacement.

B. Mid-frequency range

Increase in voltage and current magnitudes with frequency is also seen in this frequency range, but with a lower slope of $+0.5$ in logarithmic scale. On the other hand, magnitude of the uncorrected charge measurement increases with an approximately $+1$ slope in logarithmic scale, whereas after correction, its slope is approximately halved since it approaches the corner frequency of the amplifier. The phases of all measured signals remain almost constant.

Coherences of charge measurements improve with frequency, becoming very close to 1 at 2 Hz. Coherences of voltage and current measurements remain close to 1 over the entire frequency range. The PRs of all signals slightly increase with frequency. Current and voltage sensings show very similar PRs, while charge sensing is slightly inferior.

Therefore, voltage and current measurements are better suited in this operational range due to better coherences and stronger signals than charge. Voltage measurement circuitry is slightly simpler to implement.

C. High-frequency range

Within this frequency range, the magnitudes and phases of all measurements remain almost constant. All three signals yield very good coherences in this frequency range. The PRs of current and voltage measurements are close to equal, and they display approximately 10 dB stronger signals than charge measurement.

Therefore, all measurement methods are usable within this frequency range. While voltage measurement is simplest to implement, measuring the charge requires circuit that is more complex to implement and yields weaker signal.

IV. CONCLUSION

This paper reports a comparative study of active IPMC sensing methods, i.e. voltage, current, and charge, in term of their frequency responses, coherences, and signal power ratios in the measurement (PR). Consistent tip displacement of 1.8 *mm* amplitude are imposed on the IPMC samples over the entire frequency interval of 0.08 Hz to 60 Hz. Each of these signals are conditioned using dedicated custom-made amplifier circuits. Sensing behaviours were analysed and compared in three frequency ranges:

- 0.08 Hz to 1 Hz: Measuring current is the best suited sensing method for this frequency range due to high signal magnitude, good coherence, and strong signal with respect to noise. Voltage measurement is simpler to implement, but it has lower coherence than current.
- 1 Hz to 10 Hz: Voltage and current measurements are well suited for this frequency range due to high coherence and PR values.
- 10 Hz to 60 Hz: In this frequency range, all measurement methods are usable.

ACKNOWLEDGMENT

This project has been supported financially by Malaysia Ministry of Higher Education (MOHE) and University Malaysia Pahang (UMP), Malaysia under Skim Latihan Akademik Bumiputra (SLAB) scholarship program.

REFERENCES

[1] Z. Chen, "A review on robotic fish enabled by ionic polymer–metal composite artificial muscles," *Robotics and Biomimetics*, vol. 4, no. 1, p. 24, Dec 2017.

[2] Y. Xin *et al.*, "The use of polyvinylidene fluoride (pvdf) films as sensors for vibration measurement: A brief review," *Ferroelectrics*, vol. 502, no. 1, pp. 28–42, 2016.

[3] C. Li *et al.*, "Flexible dome and bump shape piezoelectric tactile sensors using pvdf-trfe copolymer," *Journal of Microelectromechanical Systems*, vol. 17, no. 2, pp. 334–341, April 2008.

[4] F. Bauer *et al.*, "Recent advances in highly electrostrictive p(vdf-trfe-cfe) terpolymers," *IEEE Trans. on Dielectrics and Electrical Insulation*, vol. 13, no. 5, pp. 1149–1154, Oct 2006.

[5] *DuraAct^{TM}–Piezoelectric Patch Transducers for Industry and Research*, DuraAct, Physik Instrumente GmbH, 2007.

[6] L. He, J. Lou, J. Du, and J. Wang, "Finite bending of a dielectric elastomer actuator and pre-stretch effects," *International Journal of Mechanical Sciences*, vol. 122, pp. 120 – 128, 2017.

[7] K. Kaneto, "Research trends of soft actuators based on electroactive polymers and conducting polymers," *Journal of Physics: Conference Series*, vol. 704, no. 1, p. 012004, 2016.

[8] M. Shahinpoor and K. J. Kim, "Ionic polymer-metal composites: I. fundamentals," *Smart Mat. Struct.*, vol. 10, no. 4, p. 819, 2001.

[9] M. ul Haq and Z. Gang, "Ionic polymer–metal composite applications," *Emerging Materials Research*, vol. 5, no. 1, pp. 153–164, 2016.

[10] K. Sadeghipour, R. Salomon, and S. Neogi, "Development of a novel electrochemically active membrane and 'smart' material based vibration sensor/damper," *Smart Mat. Struct.*, vol. 1, no. 2, pp. 172–179, Jun. 1992.

[11] A. Hunt, Z. Chen, X. Tan, and M. Kruusmaa, "Feedback Control of a Coupled IPMC (Ionic Polymer-Metal Composite) Sensor-Actuator," in *ASME 2009 Dynamic Systems and Control Conference, Volume 1*, California, USA, Sep. 2009, pp. 485–491.

[12] T. Ganley *et al.*, "Temperature-dependent ionic polymer-metal composite (IPMC) sensing dynamics: Modeling and inverse compensation," *IEEE/ASME International Conference on Advanced Intelligent Mechatronics, AIM*, pp. 447–452, 2010.

[13] ——, "Modeling and inverse compensation of temperature-dependent ionic polymer-metal composite sensor dynamics," *IEEE/ASME Transactions on Mechatronics*, vol. 16, no. 1, pp. 80–89, 2011.

[14] K. M. Newbury and D. J. Leo, "Electromechanical modeling and characterization of ionic polymer benders," *Journal of Intelligent Material Systems and Structures*, vol. 13, no. 1, pp. 51–60, 2002.

[15] ——, "Linear Electromechanical Model of Ionic Polymer Transducers – Part I : Model Development," *Journal of Intelligent Material Systems and Structures*, vol. 14, no. 6, pp. 333–342, 2003.

[16] C. Bonomo, L. Fortuna, P. Giannone, S. Graziani, and S. Strazzeri, "A model for ionic polymer metal composites as sensors," *Smart Mater. Struct.*, vol. 15, no. 3, pp. 749–758, 2006.

[17] S. Nemat-Nasser and J. Y. Li, "Electromechanical response of ionic polymer-metal composites," *J. of Applied Physics*, vol. 87, no. 7, pp. 3321–3331, 2000.

[18] S. Nemat-Nasser, "Micromechanics of actuation of ionic polymer-metal composites," *J. Appl. Phys.*, vol. 92, no. 5, pp. 2899–2915, 2002.

[19] K. Farinholt and D. J. Leo, "Modeling of electromechanical charge sensing in ionic polymer transducers," *Mechanics of Materials*, vol. 36, no. 5, pp. 421–433, 2004.

[20] K. M. Farinholt, "Modeling and Characterization of Ionic Polymer Transducers for Sensing and Actuation," Ph.D. dissertation, Virginia Polytechnic Institute and State University, VA, USA, november 2005.

[21] Z. Chen *et al.*, "A dynamic model for ionic polymer–metal composite sensors," *Smart Mater. Struct.*, vol. 16, no. 4, pp. 1477–1488, 2007.

[22] Z. Chen, "Ionic polymer-metal composite artificial muscles and sensors: A control systems perspective," Ph.D. dissertation, Michigan State University, Michigan, USA, 2009.

[23] M. Porfiri, "An electromechanical model for sensing and actuation of ionic polymer metal composites," *Smart Mater. Struct.*, vol. 18, no. 1, p. 015016, 2008.

[24] M. Aureli and M. Porfiri, "Nonlinear sensing of ionic polymer metal composites," *Contin. Mech. Thermodyn.*, vol. 25, no. 2, pp. 273–310, 2013.

[25] H. Lei, C. Lim, and X. Tan, "Modeling and inverse compensation of dynamics of base-excited ionic polymer–metal composite sensors," *J. Intel. Mat. Sys. Struct.*, vol. 24, no. 13, pp. 1557–1571, 2013.

[26] A. McDaid *et al.*, "A compliant surgical robotic instrument with integrated ipmc sensing and actuation," *International Journal of Smart and Nano Materials*, vol. 3, no. 3, pp. 188–203, 2012.

[27] H. Lei *et al.*, "Dynamics of omnidirectional IPMC sensor: Experimental characterization and physical modeling," *IEEE/ASME Transactions on Mechatronics*, vol. 21, no. 2, pp. 601–612, 2016.

[28] M. Konyo *et al.*, "Development of velocity sensor using ionic polymer-metal composites," in *Proc.SPIE*, vol. 5385, CA, USA, july 2004.

[29] A. Etebari *et al.*, "A dynamic wall shear stress sensor based on ionic polymers," in *ASME. Fluids Engineering Division Summer Meeting*, vol. 2:Fora.

[30] B. Ando *et al.*, "A seismic sensor based on IPMC combined with ferrofluids," *IEEE Transactions on Instrumentation and Measurement*, vol. 62, no. 5, pp. 1292–1298, 2013.

[31] B. Paola *et al.*, "Ipmcs as vibration sensors," in *2008 IEEE Instr. Meas. Tech. Conf.*, May 2008, pp. 2065–2069.

[32] C. Gonzalez and R. Lumia, "An ipmc microgripper with integrated actuator and sensing for constant finger-tip displacement," *Smart Materials and Structures*, vol. 24, no. 5, p. 055011, 2015.

[33] H. Lei *et al.*, "Performance improvement of ipmc flow sensors with a biologically-inspired cupula structure," vol. 9798, 2016.

[34] E. Esmaeli, M. Ganjian, H. Rastegar, M. Kolahdouz, Z. Kolahdouz, and G. Q. Zhang, "Humidity sensor based on the ionic polymer metal composite," *Sensors and Actuators, B: Chemical*, vol. 247, pp. 498–504, 2017.

[35] Y. Ming *et al.*, "Ipmc sensor integrated smart glove for pulse diagnosis, braille recognition, and human–computer interaction," *Advanced Materials Technologies*, vol. 3, no. 12, p. 1800257, 2018.

[36] M. Shahinpoor, Y. Bar-Cohen, J. O. Simpson, and J. Smith, "Ionic polymer-metal composites (IPMCs) as biomimetic sensors, actuators and artificial muscles - a review," *Smart Mat. Struct.*, vol. 7, no. 6, pp. R15–R30, 1998.

[37] K. Newbury, "Characterization , Modeling , and Control of Ionic Polymer Transducers," Ph.D. dissertation, Virginia Polytechnic Institute and State University, Blacksburg, september 2002.

[38] C. Bonomo, C. D. Negro, L. Fortuna, and S. Graziani, "Characterization of ipmc strip sensorial properties: preliminary results," in *Proceedings of the 2003 International Symposium on Circuits and Systems, 2003. ISCAS '03.*, vol. 4, May 2003, pp. IV–IV.

[39] X. Chew, a. V. D. Hurk, and K. Aw, "Characterisation of ionic polymer metallic composites as sensors in robotic finger joints," *International Journal of Biomechatronics and Biomedical Robotics*, vol. 1, no. 1, pp. 37 – 43, 2009.

[40] Z. Zhu, T. Horiuchi, K. Kruusamäe, L. Chang, and K. Asaka, "The effect of ambient humidity on the electrical response of ion-migration-based polymer sensor with various cations," *Smart Materials and Structures*, vol. 25, no. 5, p. 055024, 2016.

[41] C. Bonomo, L. Fortuna, P. Giannone, S. Graziani, and S. Strazzeri, "A resonant force sensor based on ionic polymer metal composites," *Smart Materials and Structures*, vol. 17, no. 1, p. 015014, 2008.

[42] A. Hunt, Z. Chen, X. Tan, and M. Kruusmaa, "An integrated electroactive polymer sensor–actuator: design, model-based control, and performance characterization," *Smart Materials and Structures*, vol. 25, no. 3, p. 035016, 2016.

[43] A. Hunt, "Application-Oriented Performance Characterization of the Ionic Polymer Transducers (IPTs)," Ph.D. dissertation, Tallinn University of Technology, Tallinn, april 2017.

[44] M. D. Bennett and D. J. Leo, "Ionic liquids as stable solvents for ionic polymer transducers," *Sensors and Actuators, A: Physical*, vol. 115, no. 1, pp. 79–90, 2004.

[45] D. Griffiths, J. Dominic, B. J. Akle, P. P. Vlacho, and D. J. Leo, "Development of ionic polymer transducers as flow shear stress sensors: effects of electrode architecture," in *Proc.SPIE*, vol. 6529, California, USA, apr 2007, p. 65290L.

[46] M. Gudarzi, P. Smolinski, and Q. M. Wang, "Bending mode ionic polymer-metal composite (IPMC) pressure sensors," *Measurement: Journal of the International Measurement Confederation*, vol. 103, no. February, pp. 250–257, 2017.

[47] C. Bonomo, L. Fortuna, P. Giannone, and S. Graziani, "A method to characterize the deformation of an ipmc sensing membrane," *Sensors and Actuators A: Physical*, vol. 123-124, pp. 146 – 154, 2005, eurosensors XVIII 2004.

[48] A. Punning, M. Kruusmaa, and A. Aabloo, "Surface resistance experiments with ipmc sensors and actuators," *Sensors and Actuators A: Physical*, vol. 133, no. 1, pp. 200 – 209, 2007.